Available online at www.sciencedirect.com
ScienceDirect
Trans. Nonferrous Met. Soc. China 35(2025) 1338−1349
Transactions of Nonferrous Metals Society of China
www.tnmsc.cn

Enhanced separation of yttrium, erbium and thulium with P507 induced by complexation kinetics of DTPA

Na SUI[1,2], Shu-kai MIAO[1], Hao SHEN[1], Kai-hui CUI[1], Jia-qi WANG[1], Kun HUANG[1]

1. School of Metallurgical and Ecological Engineering,
University of Science and Technology Beijing, Beijing 100083, China;
2. Key Laboratory of Ionic Rare Earth Resources and Environment,
Ministry of Natural Resources, Ganzhou 341000, China

Received 18 September 2023; accepted 1 March 2024

Abstract: Based on a non-equilibrium kinetic extraction technique, the complexation kinetics of diethylenetriaminepentaacetic acid (DTPA) with rare earth (RE) ions was investigated with different adding sequences of DTPA. The results indicated that the separation factors of $\beta_{Tm/Er}$ and $\beta_{Y/Er}$ were higher when adding DTPA at the start of extraction than those before extraction. The extraction order for Y, Er and Tm was Tm>Y>Er. The root of discrepancy in complexation kinetics of Y, Er and Tm ions with DTPA and the enhanced kinetic separation mechanism were elucidated from the forward complex formation and reverse dissociation rates by the stopped-flow spectrophotometric technique. The apparent complexation rate constants began to decrease gradually with the increase of aqueous pH, while increased with increasing DTPA concentration. The emergence of extraction priority order as Tm>Y>Er was verified according to the calculated reaction kinetic constants of Y, Er and Tm at different pH values.

Key words: rare earths; extraction; complexation kinetics; diethylenetriaminepentaacetic acid (DTPA); stopped-flow spectrophotometric technique

1 Introduction

The demand for heavy rare earths (HREs) exceeds a quarter of the demand for total rare earths, which highlights the strategic position of HREs. It is known that the mutual separation of HREs into an individual element is extremely difficult [1,2]. The difficulty lies in their co-existence as well as similar physicochemical properties [3].

Solvent extraction is still efficient for the enrichment and mutual separation of REs [4−7]. In the conventional extraction technology, the separation of Y from high-yttrium ore is first carried out by naphthenic acid and then the separation of other REs by P507. As a secondary product of the petroleum processing industry, the output of naphthenic acid is limited and the supply as the extractant cannot be guaranteed. It is imperative to exploit an alternative extraction system to replace naphthenic acid. As reported, the leaching solution of high-yttrium ore was firstly divided into Er/Tm groups with P507-isooctanol followed by separating Y from the high Y-enrichment of Er group with sec-octylphenoxy acetic acid (CA12)-tri-n-butyl phosphate (TBP) [8]. The enhanced kinetic separation of Er/Tm on the surface of freely rising oil droplets to simultaneously control the separation order of Y has been achieved only requiring the extractant of P507 based on the complexation extraction [9]. The study of coordination chemistry is essential for efficient extraction of metal ions

Corresponding author: Kun HUANG, Tel: +86-13811873892, E-mail: huangkun@ustb.edu.cn
DOI: https://doi.org/10.1016/S1003-6326(24)66752-X

[10,11]. The water-soluble complexing agent has a function of masking a certain metal ion, which allows the selective extraction of other metal ions. The previous research about the complexation extraction of HREs was mainly focused on the complexation and extraction thermodynamics [12,13]. The separation of Y(III), Ho(III), Er(III) was strengthened when existing EDTA, based on different complexation stability constants between different RE ions and EDTA [14]. Due to the masking effect from EDTA or DTPA, the selective extraction of Y from heavy lanthanides was enhanced by CA-100 [15].

The rare-earth complexation kinetics has a great impact on their enhanced separation [16]. The RE−DTPA complex formation rate is very fast [17]. However, RE−DTPA complex dissociation rate is relatively slow [18]. The complexation kinetics has been investigated adopting a kind of techniques such as spectrophotometry [19], and NMR spectroscopy [20]. For these techniques, the rates of complex formation are too fast to analyze and detect for obtaining the accurate kinetic data to explain complexation kinetic discrepancy. And thus, how to realize fast online detection is crucial to finding out the mechanism of complexation kinetic separation for rare earths difficult to be separated. The stopped-flow technique is applicable to the complexation reactions occurring in a short time regime, which has been confirmed to be efficient for kinetics research about homogeneous reactions on the basis of its advantages including but not limited to small solvent consumption and easy operation. Complexation rate differences of lanthanides with EDTA and DTPA were successfully monitored and analyzed by stopped-flow spectrophotometry [21,22]. The regulation behaviors of absorption kinetics of CO_2 were elucidated and rapid chlorination rate constants were acquired by the stopped-flow technique [23−25]. There is less investigation into complexation kinetics of Er, Tm and Y with DTPA by the stopped-flow technique, especially for the competitive complexation which occurs between the complexing agent and the extractant.

Based on the discrepancy in extraction and mass transfer rates, the mutual separation of multiple rare earths can be improved at a non-equilibrium state. By non-equilibrium kinetic separation, the separation of components difficult to be separated can be enhanced. The production costs are also reduced. Compared to the disadvantage of more extraction stages in the conventional extraction, the extraction stages decrease significantly by a kinetic separation method. The energy consumption is also reduced. According to the previous work, the enhanced kinetic separation of Er/Tm and simultaneously controlling the separation order of Y was achieved by a kinetic separation method. However, the enhanced separation mechanism of HREs by the complexation extraction has not been clearly explained at a non-equilibrium state. The present work aims at in-depth exploration about the mechanism of enhanced separation by the complexation extraction at a non-equilibrium state. The complexation kinetics of DTPA with Y, Er and Tm ions under different added sequences of DTPA is explained from the forward complex formation and reverse dissociation processes by stopped-flow technique. This research provides a theoretical foundation for adjusting the order of Y between Er and Tm to help achieve the enhanced grouping of Er and Tm and solve the problem of Y extraction simultaneously.

2 Experimental

2.1 Reagents and materials

The extractant of 2-ethylhexyl phosphonic acid mono (2-ethylhexyl) ester (P507, purity ≥99 vol.%) was purchased from Shanghai Laiyashi Chemical Co., Ltd., China. The organic phase was prepared by diluting P507 using the organic solvent n-heptane. The complexing agent of DTPA was purchased from Beijing Mreda Technology Co., Ltd., China. Thulium oxide (Tm_2O_3), erbium oxide (Er_2O_3) and yttrium oxide (Y_2O_3) were purchased by Changchun Haipuri Fine Chemical Co., Ltd., China.

2.2 Experimental device and process

The concentrations of Y, Er, Tm in feed liquids were all 1 mmol/L. DTPA was employed to coordinate RE ions at the start of extraction or before extraction. The concentrations of P507 in organic phase and DTPA in the stock solution were 0.1 mol/L and 1 mmol/L, respectively. The desired pH values were measured by pH meter (pHs–3C, Beijing Gallop High&New Tech. Co., Ltd., China).

The schematic diagram of freely rising oil droplet extraction setup was depicted as our previous work [26]. After adding feed solution, 0.65 mL of DTPA stock solution was quickly driven into the extraction column with a syringe at the extraction column bottom. At the start of extraction, the oil droplets were drummed into the column with a constant rate of 0.3 mL/min. An automatic sampler was used to collect organic phase every 15 min, and 4.5 mL organic phase was collected in one sample tube for each time.

The complexation kinetics of RE ions with DTPA was studied by the stopped-flow spectrophotometry (SX20, UK) [22]. To facilitate monitoring the process of complexation between DTPA and RE(III) and dissociation behaviors of RE-DTPA, the rare earth ions were complexed by Arsenazo III (AZIII) in advance. The maximum absorption wavelength of RE−AZIII is 652 nm. An OLIS RSM Robust Global Fitting software package was used for analysis of the absorbance data as a function of time at the wavelength of 652 nm [27]. The apparent complexation reaction rate constant (A) was obtained by fitting the absorbance data following Eq. (1) [24]:

$$A = -a\exp(-k_{obs}t) + A_{\infty} \tag{1}$$

where A represents the absorbance; a and A_{∞} are the coefficient of the curve and constant value obtained by fitting; k_{obs} is the rate constant for complexation reaction, which can be automatically generated based on the typical graph versus time using Kinetasyst software.

Secondary analysis of data correlating observed rate constants with ligand concentration was conducted using Origin 2021, as given in Eq. (2):

$$k_{obs} = k_f \cdot [\mathrm{DTPA}] + k_d \tag{2}$$

where k_f denotes the RE−DTPA complex formation rate constant, $\mathrm{L\cdot mol^{-1}\cdot s^{-1}}$; k_d is regarded as the dissociation reaction rate constant, $\mathrm{s^{-1}}$.

All experiments were performed at 25 °C.

2.3 Data analysis

The mass concentrations of RE ions in the aqueous phase were detected by the inductively coupled plasma optical emission spectrometer (ICP-OES, PerkinElmer, Optima 7000). Based on this, the concentrations of RE ions in the organic phase were calculated by the mass balance.

The extraction rate (E) of RE ions, the distribution ratio (D) between organic and aqueous phases as well as the separation coefficient (β) of different RE ions could be obtained as Eqs. (3)−(5):

$$E = 100\% - \frac{c_{a,t}}{c_{a,0}} \times 100\% \tag{3}$$

$$D = \frac{(c_{a,0} - c_{a,t})V_a}{c_{a,t}V_o} \tag{4}$$

$$\beta_{1/2} = \frac{D_1}{D_2} \tag{5}$$

where $c_{a,0}$ and $c_{a,t}$ denote initial concentration of one RE ion in feed liquid and that in aqueous phase at time t; V_o and V_a denote volumes of organic and aqueous phases, respectively; $\beta_{1/2}$ represents the separation coefficient of two different RE ions.

2.4 MD simulations

The MD simulations were realized using GROMACS 2021 program [28]. The simulation boxes were designed as 50 Å × 50 Å × 50 Å and 50 Å × 50 Å × 20 Å by PACKMOL [29]. Two oil phase boxes were placed at each end of the water phase box. The component information in the simulation boxes was listed in Table 1. The force field of OPLS-AA was used for demonstrating organic components [30]. The force field of salt and metal ions was designated as the previous literature [31]. The SPC/E model was employed for H_2O molecule [32].

For MD simulations, the temperature and pressure were controlled at 298 K and 1×10^5 Pa using a Nose−Hoover thermostat [33,34] and Parrinello−Rahman barostat [35]. To keep the box

Table 1 Details of components in MD simulation boxes

System	Number									Simulation box/nm^3
	P507	DTPA	n-heptane	Y(III)	Er(III)	Tm(III)	H_3O^+	Cl^-	Water	
Without DTPA	40	0	450	10	10	10	9	99	4000	5×5×5
With DTPA	40	10	450	10	10	10	9	99	4000	5×5×5

size unchanging, isotropic barostat coupling was adopted. Firstly, the energy minimization before the simulations was done by adopting the steepest descent algorithm. Secondly, 2 ns of NPT and NVT ensembles were employed for collecting the system equilibration. Finally, MD simulations were conducted and continued for 20 ns. Based on the results of MD simulations, the mean square distance (MSD) was obtained to interpret diffusion mass transfer rates.

3 Results and discussion

3.1 Effect of DTPA adding sequence

For further exploring the regulation of the complexation and dissociation behaviors between RE ions and DTPA on RE extraction and separation, the effect of DTPA adding order was investigated. In Figs. 1(a−c), extraction rates of RE ions were higher when adding DTPA at start of extraction than that before extraction. From Fig. 1(d), the max differences of extraction rates of different RE ions between adding DTPA at the start of extraction and before extraction reached 7.86%, 8.75% and 7.37%, respectively. It can be seen that the adding order of DTPA presented a significant effect on RE extraction. Besides, from Figs. 1(e, f), the difference between extraction rates of Tm and Er were higher when adding DTPA at the start of extraction than that before extraction. This was also the same case for Y and Er. When adding DTPA before extraction, the extraction of RE ions was related to both of complex dissociation and the RE extraction. Due to the pre-complexation of DTPA with RE ion, the RE−DTPA complexes were mainly dissociated during the extraction process. The dissociated free

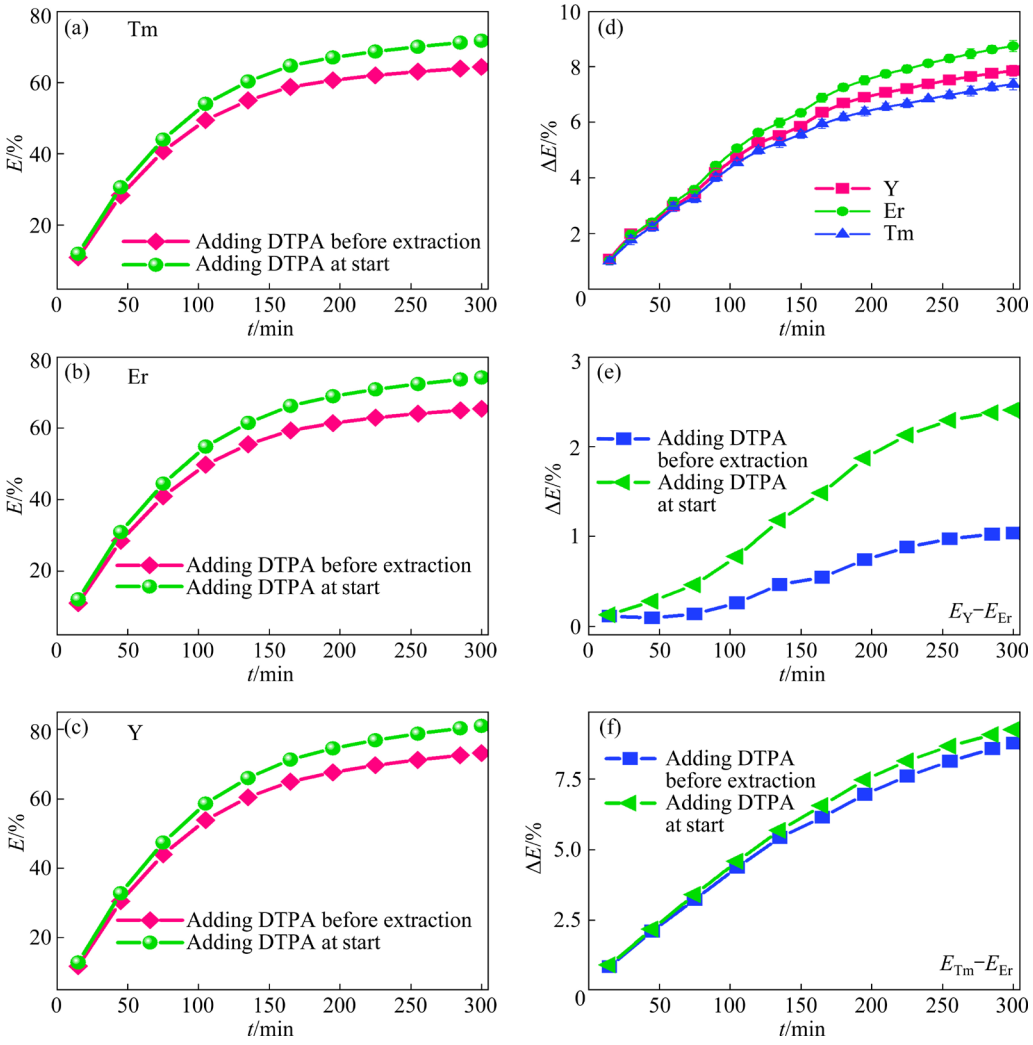

Fig. 1 Effect of adding sequence of DTPA in aqueous phase on extraction behaviors of rare earths: (a−c) Extraction rates of Y, Er and Tm; (d) Difference of extraction rates between adding DTPA at start of extraction and before extraction; (e, f) Difference of extraction rates between Y and Er, Tm and Er ([RE^{3+}]=1 mmol/L, [DTPA]=0.01 mmol/L, [P507]=0.1 mol/L, Q_{P507}=0.3 mL/min, and pH=3)

RE ions were further extracted by P507, which promoted the extraction between P507 and RE ions. When adding DTPA at the start, RE extraction was related with not only the extraction of RE ions and RE−DTPA complex dissociation but also the complex formation between RE ions and DTPA. Rapid complexation of DTPA with free RE ions occurred. Simultaneously, a part of RE ions were extracted. It was worth noting that the extraction of free ions was easier and faster when adding DTPA at the start than that dissociated from RE−DTPA complexes when adding DTPA before extraction. Therefore, the extraction rates were higher when adding DTPA at the start than that before extraction.

The extraction behaviors with different adding orders of DTPA were related to the complexation and dissociation rates between DTPA and RE ions. From Fig. 2, $\beta_{Y/Er}$ was greater when adding DTPA at the start than that before the extraction. When DTPA was added before the extraction, the separation behaviors of Y/Er were related with the extraction rate of P507 and difference in the dissociation rate of Y−DTPA and that of Er−DTPA. The dissociation rate of Y−DTPA was faster than Er−DTPA, which was related with the interaction between Y or Er and DTPA [36]. The complexation rate between Y and DTPA was slower than that of Er. In addition, by comparing the complex dissociation rate with the extraction rate, the complexation rate between DTPA and Y or Er was quite different. Therefore, when adding DTPA at the start, the complexation with DTPA was dominant. $\beta_{Tm/Er}$ was larger and the maximum value was 1.8. From the results, difference of complexation kinetics for different RE ions was important for enhancing mutual separation of RE ions.

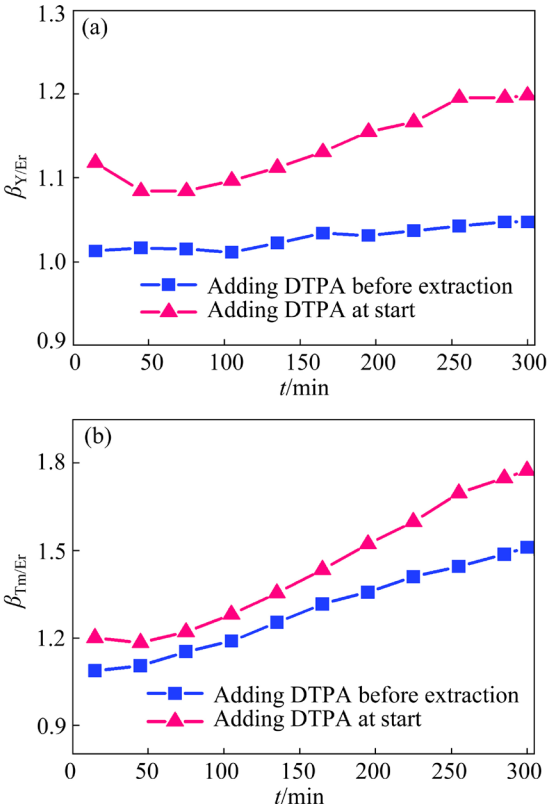

Fig. 2 Effect of adding sequence of DTPA on $\beta_{Y/Er}$ (a) and $\beta_{Tm/Er}$ (b) ([RE^{3+}]=1 mmol/L, [DTPA]=0.01 mmol/L, [P507]=0.1 mol/L, Q_{P507}=0.3 mL/min, and pH=3)

3.2 Effect of aqueous pH on apparent reaction rate constant

On one hand, the complexation kinetics between RE ions and DTPA is connected with the aqueous pH, which directly affects the complexation reaction equilibrium. The apparent complexation reaction rate constant can be used to elucidate the complexation kinetics. The effect of aqueous pH on complexation kinetics was investigated by adopting stopped-flow spectroscopy. In Figs. 3(a−c), the absorbance of Y−AZIII, Er−AZIII and Tm−AZIII complexes at λ_{max}=652 nm descended rapidly within 0.5 s. This demonstrated that the complexation between RE ions and DTPA took place. In addition, when the complexation reaction reached equilibrium at 1.5 s, the absorbance of the complexes increased with the increase of pH, which was related to different amounts of rare earth complexes at different pH values. The curves obtained in the experiments were fitted based on Eq. (1). The apparent reaction rate constant (k_{obs}) between RE ions and DTPA was obtained. From Fig. 3(d), the apparent reaction rate constants of Y, Er, Tm with DTPA gradually decreased with the increase of pH because DTPA is a five-membered weak acid (H_5D). The species distribution behaviors of H_5D were different at different pH values. At pH=2.5, DTPA existed mainly as H_4D^-. At pH=3.0, DTPA existed as H_4D^- and H_3D^{2-} coexisting in the aqueous solution. When pH=3.6, DTPA mainly existed in the form of H_3D^{2-} [37]. Therefore, during the complexation between RE ions and DTPA, it involved not only the complexation reaction, but also the ionization behavior of DTPA. The ionization rate of DTPA decreased with the increase of pH, and thus the complexation with RE ions was limited.

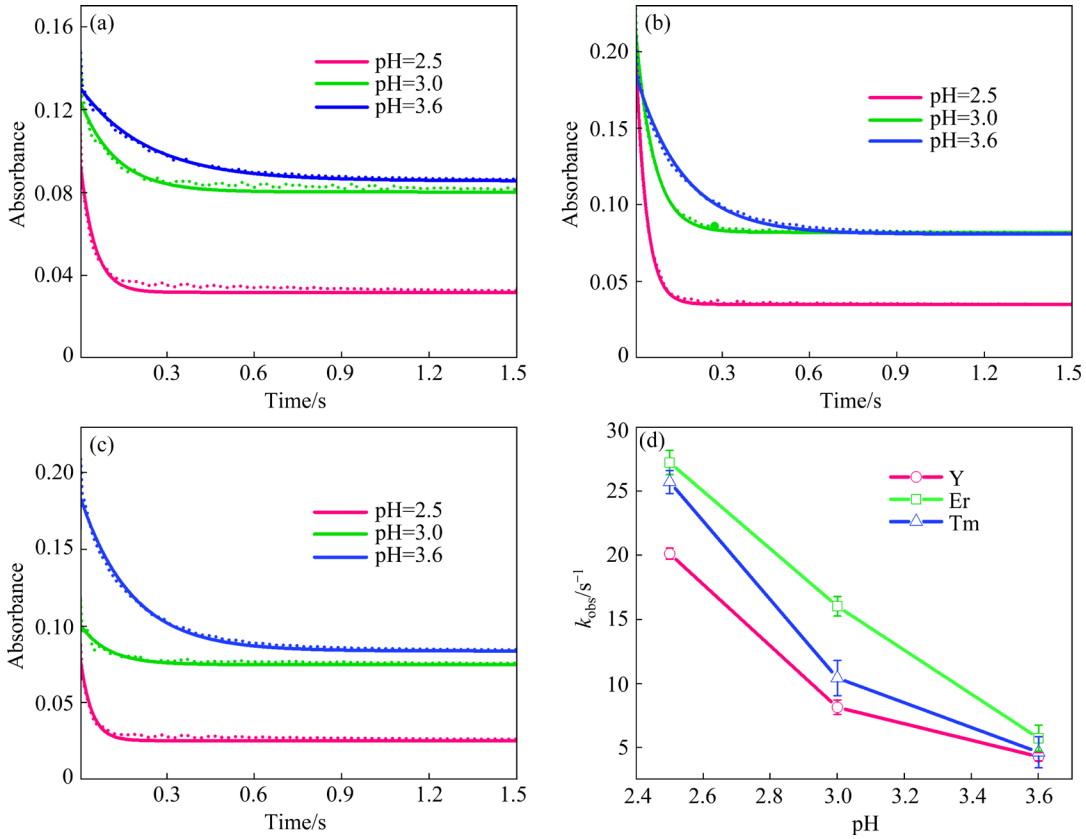

Fig. 3 Effect of pH on apparent reaction of rare earth ions with DTPA: (a) Y−DTPA complex; (b) Er−DTPA complex; (c) Tm−DTPA complex; (d) Apparent reaction rate constants of Y, Er, Tm ions with DTPA ([RE^{3+}]= 0.004 mmol/L, [DTPA]=0.06 mmol/L, ionic strength (NaCl) μ=0.2 mol/L, and λ=652 nm)

As most of RE ions existed in the form of $REHD^-$ under the condition of pH=2.5, $REHD^-$ and RED^{2-} coexisted when pH=3.0, while RED^{2-} was the main reaction product when pH>3.6. With the decrease of the aqueous acidity, H^+ in the rare earth complexes gradually dissociated. The $REHD^-$ complexes deprotonated to form RED^{2-}. The deprotonation degree increased with the decrease of the acidity, resulting in a decrease in the reaction rate. When the acidity decreased, a large amount of $REHD^-$ formed more stable RED^{2-}. Moreover, the dissociation of H^+ further resulted in a decrease in the apparent reaction rate of RE ions with DTPA. In addition, Fig. 3(d) showed that the apparent reaction rates of RE ions and DTPA conformed to Tm>Er>Y in the pH range from 2.5 to 3.6. The order was consistent with thermodynamic stability constants. In particular, at pH 3.0, the larger difference of apparent reaction rates of Tm and Er could be found. Therefore, the increase of aqueous acidity facilitated Tm/Er separation in the extraction system. When pH was 2.5, it was conducive to Y/Tm separation.

3.3 Effect of DTPA concentration on apparent reaction rate constant

On the other hand, the complexation kinetics of RE ions has a close relationship with the added DTPA concentration, which also affects the complexation reaction equilibrium. From Fig. 4, when DTPA concentration exceeded 0.05 mmol/L, the absorbance corresponding to the complexation equilibrium of Y, Er, Tm with DTPA showed an obvious upward shift. In our opinion, the concentration of complexes formed between RE ions and DTPA changed in the process of rapid complexation. The apparent reaction rate constants were obtained by fitting absorbance data change over time of 0.005−2 s.

From Fig. 5, the apparent reaction rate between RE ions and DTPA gradually increased. When DTPA concentration was in the range of 0.01−0.04 mmol/L, the apparent reaction rate of DTPA increased rapidly. There was no significant difference in the reaction rates of Y, Er and Tm. When the DTPA concentration was greater than 0.04 mmol/L, the apparent reaction rate of Er

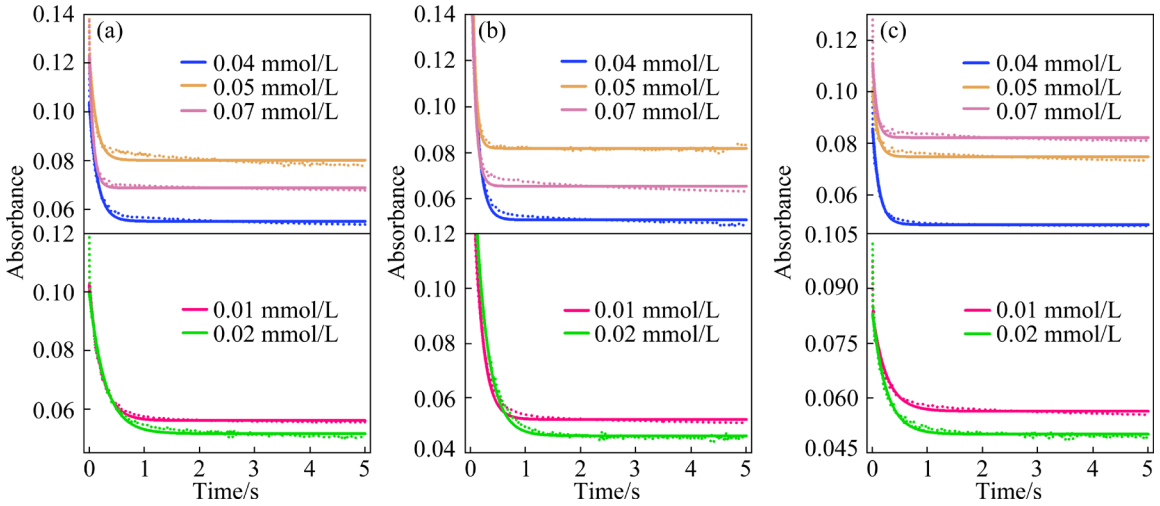

Fig. 4 Effect of DTPA concentration on absorbance of RE−DTPA complexes: (a) Y−DTPA complex; (b) Er−DTPA complex; (c) Tm−DTPA complex ([RE^{3+}]=0.004 mmol/L, pH=3, μ=0.2 mol/L, and λ=652 nm)

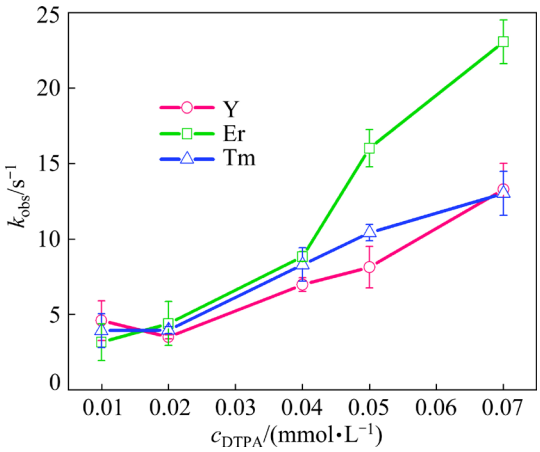

Fig. 5 Effect of DTPA concentration on apparent reaction rate constant ([RE^{3+}]=0.004 mmol/L, pH=3, μ=0.2 mol/L, and λ=652 nm)

increased rapidly, reaching the maximum value with the DTPA concentration of 0.07 mmol/L, followed by Tm and then Y. It could be seen that increasing DTPA concentration can widen the difference in reaction rates of RE ions. And thus, the enhanced separation of Er/Tm can be effectively realized.

3.4 Complexation kinetics of DTPA with rare earth ions based on stopped-flow spectrophotometry

The complexation kinetics can be determined according to the complex formation rates and the dissociation rates of the complexes. To find out the mechanism of enhanced separation of RE ions, the regulation law for the complexation kinetics involving the complexation rate and dissociation rate can be inquired by the stopped-flow spectrophotometry.

To obtain the kinetic parameters of the reaction process between RE ions and DTPA, the curves were fitted based on Eq. (2). As shown in Fig. 6, all complexation rates (k_{obs}) increased when increasing DTPA concentration. It decreased with the increase of aqueous pH from 2.5 to 3.6. The complex formation and dissociation rates were different under different pH conditions. In order to facilitate interpretation of the complexation kinetics, the effect of aqueous pH on k_f and k_d were analyzed, respectively.

As shown in Fig. 7, in the pH range of 2.5−3.6, the complexation rate between RE ion and DTPA gradually decreased with the increase of pH. This was because DTPA gradually deprotonated to form a more stable H_3D^{2-} within this range, resulting in a decline in the complexation reaction rate between RE ions and DTPA [38]. It could be seen that the protonation degree of DTPA had a significant effect on the complexation rate of RE ions from Fig. 7(a). In addition, the complexation rate of Er was faster than that of Y and Tm, which indicated that the forward complexation reaction between Er and DTPA was dominant when adding DTPA at the start. The complexation rate of Er was greater than that of Tm. When increasing aqueous pH, the complexation rate of Er decreased rapidly. From Fig. 7(b), the dissociation rate of Er−DTPA was the highest at pH=2.5, which was different from the complexation rate. Under this condition, there were more free Tm ions. This was also the reason why

the extraction rate of Er was the fastest at pH=2.5.

The details of the rare earth complexation and deionization rate constants with DTPA are listed in Table 2. When DTPA was added, RE extraction rate was obviously influenced by aqueous acidity. This was because the acidity had an obvious influence on the complexation with DTPA and RE−DTPA dissociation behaviors. Therefore, it is very necessary to strictly control the initial aqueous pH value in the process of regulating the separation of RE ions. Besides, it was worth noting that the dissociation rate constant of Y−DTPA complexes increased obviously at pH=3.0. Compared with Er^{3+} and Tm^{3+}, it was known that the complexation stability constant of Y^{3+} with DTPA was lower. It could be concluded that the complexation reaction between Y^{3+} and DTPA mainly occurred when pH was 3.0. With the increase of pH from 2.5 to 3.0, the complexation reaction between Y^{3+} and DTPA was promoted. The product of Y−DTPA complexes increased. The dissociation of the complexes was also promoted. Therefore, the promotion effect on

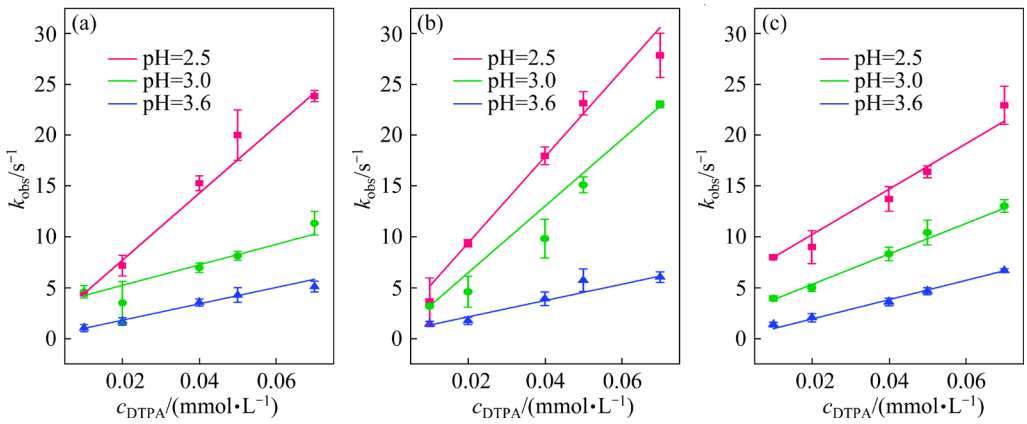

Fig. 6 Dependence of reaction rate constant on pH: (a) Y; (b) Er; (c) Tm ([RE^{3+}]=0.004 mmol/L, μ=0.2 mol/L, and λ=652 nm)

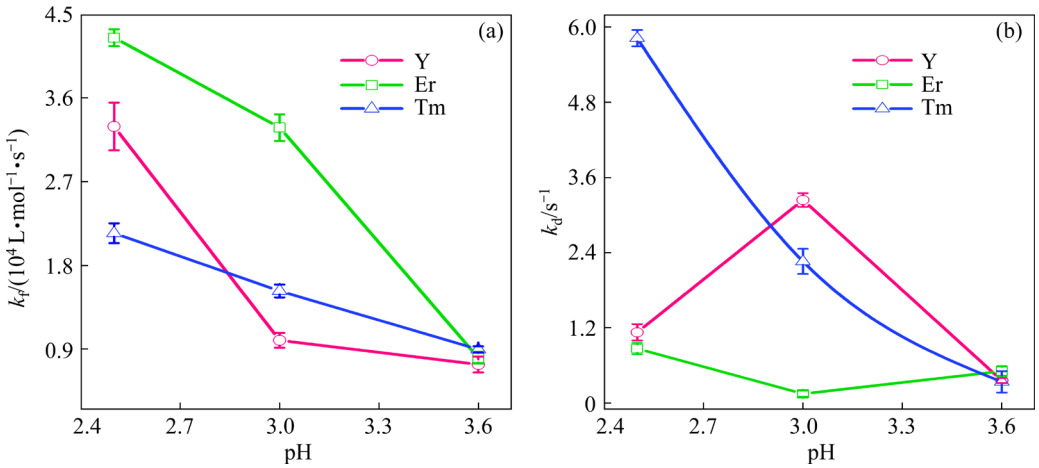

Fig. 7 Complexation and dissociation rate constants of rare earth ions with DTPA: (a) k_f; (b) k_d ([RE^{3+}]=0.004 mmol/L, μ=0.2 mol/L, and λ=652 nm)

Table 2 Complexation rate constant (k_f) and dissociation rate constant (k_d) of Y, Er and Tm with DTPA ([RE^{3+}]=1 mmol/L, [DTPA]=1 mmol/L, T=25 °C, and μ=0.1 mol/L)

Aqueous pH	Y		Er		Tm	
	$k_f/(10^3 L\cdot mol^{-1}\cdot s^{-1})$	k_d/s^{-1}	$k_f/(10^3 L\cdot mol^{-1}\cdot s^{-1})$	k_d/s^{-1}	$k_f/(10^3 L\cdot mol^{-1}\cdot s^{-1})$	k_d/s^{-1}
2.5	32.94	1.13	42.5	0.87	21.45	5.82
3	9.92	3.24	32.82	0.15	15.23	2.26
3.6	7.31	0.36	8.04	0.51	8.94	0.34

the dissociation of Y−DTPA complexes induced by the increase of pH dominated.

To elucidate the relationship between mass transfer behaviors of RE ions and the complexation kinetics of DTPA, MSD for RE ions was analyzed. The line slope of the MSD values was proportional to the diffusion rates. The line slope for Tm^{3+} was greater than that for Er^{3+} without DTPA, as shown in Fig. 8(a). The line slope of Er^{3+} was higher than that of Y^{3+}. It was not difficult to see that the mass transfer rate of RE ions followed a sequence of Tm>Er>Y, which was consistent with the extraction order without the complexation between DTPA and RE ions. The sequence was mainly dominated by the interaction between RE ions and extractant molecules. However, the line slope for Er^{3+} was higher than that of Tm^{3+} and Y^{3+} in Fig. 8(b). Besides, the line slope of Y^{3+} was also greater than that of Tm^{3+}. In our opinion, such mass transfer rate sequence of Er>Y>Tm was the result from comprehensive effect of the complexation with DTPA and the extraction by P507, and the complexation with DTPA played a dominant role in the mass transfer of RE ions.

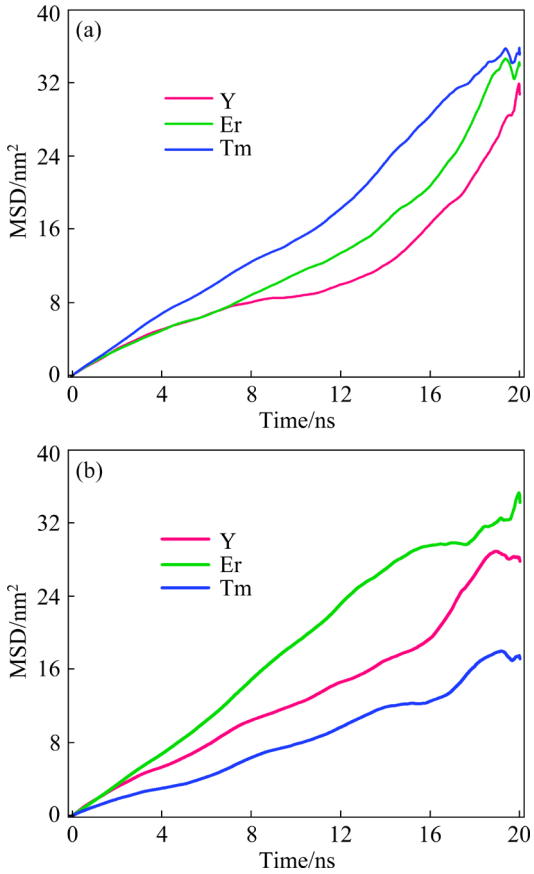

Fig. 8 MSD of Y, Er, Tm from water phase towards oil/water interface: (a) Without DTPA; (b) With DTPA

3.5 Comparison in reaction kinetic and thermodynamic equilibrium constants of Y, Er and Tm

To further quantitatively interpret the mechanism of kinetic separation, the reaction kinetic constants were calculated and compared with thermodynamic equilibrium constants. The equilibrium constant (K) of metal ion coordination is an important parameter for evaluating metal complex stability [39]. The stability constants of metal complexes are different under different conditions. However, it is necessary to consider multistage equilibrium constants of complexation reactions for polyvalent metal ions and polybasic complexants.

In the experiments of the fast complexation kinetics between RE ions and DTPA, their complexation and dissociation rate constants were determined simultaneously using stopped-flow spectrophotometry. The reaction kinetic constants of the metal complexes under specific conditions in a non-equilibrium state could be calculated by complexation and dissociation rate constants [40,41]:

$$\lg K = \lg\left(k_f / k_d\right) \tag{6}$$

The complexation processes of RE ions and DTPA were different at different aqueous pH values. The first step was the rapid stripping of rare earths from AZIII.

At pH=2.5, the complexation mainly occurred as Eq. (7):

$$RE^{3+} + H_4D^- \rightleftharpoons REHD^- + 3H^+ \tag{7}$$

According to our previous work, the molar fractions of H_4D^- and H_3D^{2-} were basically the same at pH=3.0. The molar fraction of rare earth ions participating in the complexation reaction with H_4D^- was equal to that with H_3D^{2-}. The complexation mainly occurred as Eq. (8):

$$RE^{3+} + 1/2H_3D^{2-} + 1/2H_4D^- \rightleftharpoons 1/2RED^{2-} + 1/2HRED^- + 3H^+ \tag{8}$$

At pH=3.6, the complexation mainly occurred as Eq. (9).

$$RE^{3+} + H_3D^{2-} \rightleftharpoons RED^{2-} + 3H^+ \tag{9}$$

The above equilibrium constants can be calculated making use of thermodynamic stability constants as reported in literature [42,43]. Table 3

gives the comparison between the reaction kinetic constants calculated by Eq. (6) and the thermodynamic equilibrium constants calculated by the above stability constants.

Table 3 Reaction kinetic constants and thermodynamic equilibrium constants ([RE^{3+}]=1 mmol/L, [DTPA]= 1 mmol/L, T = 25 °C, and μ=0.1 mol/L)

RE	pH=2.5		pH=3.0		pH = 3.6	
	$\lg(k_f/k_d)$	$\lg K_1$	$\lg(k_f/k_d)$	$\lg K_2$	$\lg(k_f/k_d)$	$\lg K_3$
Y	1.46	−24.05	0.49	−12.68	1.31	−1.31
Er	1.68	−23.96	2.34	−12.29	1.19	−0.62
Tm	0.57	−24.06	0.83	−12.35	1.42	−0.64

From Table 3, it could be seen that there was a great difference between the reaction kinetic constant and the thermodynamic equilibrium constant. This was mainly because the diffusion of DTPA and the hydration ability of RE ions had an influence on the complexation kinetics. When rare earth ions were dissociated from RE−AZIII complexes, the rare earth ions would first form hydrated RE ions with H_2O molecules, and then DTPA would replace H_2O from the hydrated RE ions. Besides, the changes in hydration numbers of Y and Tm (8 and 7) also had an indirect effect on kinetic behaviors of complexation. The metal ions with less hydration number were more likely to lose their coordinated solvent molecules. The smaller ions were more likely to be complexed by DTPA. In addition, when pH=2.5, the order of reaction kinetic constants was Er>Y>Tm. The discrepancy between the complexation and dissociation rates for Er was greater than that for Y, and the discrepancy of Y was greater than that of Tm. When pH=3.0, the order was changed to be Er>Tm>Y. The discrepancy in the complexation and dissociation rates for Er was greater than that of Tm, and the discrepancy of Tm was greater than that of Y. When pH=3.6, the order was changed to be Tm>Y>Er. The discrepancy in the complexation and dissociation rates for Tm was greater than that for Y, and the discrepancy of Y was greater than that of Er. From the order of reaction kinetic constants, it could be found that the complexes generated by the complexation between Tm and DTPA became more and more stable by increasing aqueous pH. This might be caused by the dissociation rate of Tm decreasing obviously. The complexation rate of Er with DTPA decreased. Moreover, since the extraction of RE by P507 was actually a process of cation exchange, raffinate pH could decrease with the gradual increase of H^+. When the order of reaction kinetic constants was Er>Y>Tm, Tm should be preferentially extracted by P507. Such an order was exactly in line with the mass transfer rate order under complexation effect of DTPA, as shown in Fig. 7(b). Finally, there occurred an extraction sequence as Tm>Y>Er.

4 Conclusions

(1) The kinetic mechanism of complexation was investigated based on a non-equilibrium kinetic extraction strategy with different added orders of DTPA. The extraction rates of Y, Er and Tm were higher when adding DTPA before extraction than those at the start of extraction. $\beta_{Y/Er}$ was higher when adding DTPA at the start than that before the extraction.

(2) By the stopped-flow spectrophotometry, the apparent rate constants gradually increased when increasing DTPA concentration, while the constants gradually decreased when increasing aqueous pH.

(3) There was a great difference between the reaction kinetic constant and the thermodynamic equilibrium constant, which could be attributed to the influence of the diffusion of DTPA and the hydration ability of RE ions on the complexation kinetics. The study lays the theoretical foundation for the application of the kinetic separation technique for purification of metal ions difficult to be separated.

CRediT authorship contribution statement

Na SUI: Investigation, Methodology, Validation, Writing − Original draft, Writing − Review & editing, Funding acquisition; **Shu-kai MIAO:** Investigation, Writing − Original draft, Validation, Writing − Review & editing; **Hao SHEN:** Data curation, Writing − Review & editing; **Kai-hui CUI:** Data curation, Resources, Software; **Jia-qi WANG:** Data curation, Validation; **Kun HUANG:** Funding acquisition, Conceptualization, Writing − Review & editing, Supervision.

Declaration of competing interest

The authors declare that they have no known competing financial interests or personal relationships

that could have appeared to influence the work reported in this paper.

Acknowledgments

This work was funded by Key Laboratory of Ionic Rare Earth Resources and Environment, Ministry of Natural Resources, China (No. 2022IRERE206) and financially supported by the National Natural Science Foundation of China (Nos. 51904027, 52074031).

References

[1] LIAO Chun-fa, NIE Hua-ping, JIAO Yun-fen, LIANG Yong, YANG Shao-hua. Study on the diffusion kinetics of adsorption of heavy rare earth with Cyanex272-P507 impregnated resin [J]. Journal of Rare Earths, 2010, 128: 120−124.

[2] LIAO Chun-fa, JIAO Yun-fen, LIANG Yong, JIANG Ping-guo, NIE Hua-ping. Adsorption−extraction mechanism of heavy rare earth by Cyanex272-P507 impregnated resin [J]. Transactions of Nonferrous Metals Society of China, 2010, 20: 1511−1516.

[3] WU Shan, BIE Chao, SU Hao, GAO Yun, SUN Xiao-qi. The effective separation of yttrium and other heavy rare earth elements with salicylic acid derivatives [J]. Minerals Engineering, 2022, 178: 107396.

[4] HIDAYAH N N, ABIDIN S Z. The evolution of mineral processing in extraction of rare earth elements using liquid−liquid extraction: A review [J]. Minerals Engineering, 2018, 121: 146−157.

[5] LIU Tian-chi, CHEN Ji. Extraction and separation of heavy rare earth elements: A review [J]. Separation and Purification Technology, 2021, 276: 119263.

[6] WANG Meng, HUANG Xiao-wei, XIA Chao, FENG Zong-yu, XU Yang, MENG De-liang, PENG Xin-lin. Efficient preparation of magnesium bicarbonate from magnesium sulfate solution and saponification−extraction for rare earth separation [J]. Transactions of Nonferrous Metals Society of China, 2023, 33: 584−595.

[7] MISHRA B B, DEVI N. Application of bifunctional ionic liquids for extraction and separation of Eu^{3+} from chloride medium [J]. Transactions of Nonferrous Metals Society of China, 2022, 32: 2061−2070.

[8] HAN Ya-xing, CHEN Ji, DENG Yue-feng, LIU Tian-chi, LI Hai-lian, LI De-qian. An innovative technique for the separation of ion-adsorption high yttrium rare earth ore by Er(III)/Tm(III) grouping first [J]. Separation and Purification Technology, 2022, 280: 119929.

[9] SONG Qiang, ZHANG Wen-jie, TONG Xiong, XIE Xian, LAN Zhuo-yue, DU Yun-peng, CAO Yang, FAN Pei-qiang. Extraction kinetics of lanthanum and cerium in bis(2-ethylhexyl) phosphate (HDEHP)-lactic acid complex system using Lewis cell [J]. Transactions of Nonferrous Metals Society of China, 2023, 33: 1943−1952.

[10] TIAN Guo-xin, RAO Lin-feng. Effect of temperature on the protonation of the TALSPEAK ligands: Lactic and diethylenetrinitropentaacetic acids [J]. Separation Science and Technology, 2010, 45: 1718−1724.

[11] SUN Xiao-qi, DO-THANH C L, LUO Hui-min, DAI Sheng. The optimization of an ionic liquid-based TALSPEAK-like process for rare earth ions separation [J]. Chemical Engineering Journal, 2014, 239: 392−398.

[12] GRIMES T S, NASH K L. Acid dissociation constants and rare earth stability constants for DTPA [J]. Journal of Solution Chemistry, 2014, 43: 298−313.

[13] NISHIHAMA S, SAKAGUCHI N, HIRAI T, KOMASAWA I. Extraction and separation of heavy rare earth metals in the presence of diethylenetriaminepentaacetic acid [J]. Solvent Extraction Research and Development−Japan, 2000, 7: 159−166.

[14] NISHIHAMA S, SAKAGUCHI N, HIRAI T, KOMASAWA I. Selective extraction of Y from a Ho/Y/Er mixture by liquid-liquid extraction in the presence of a water-soluble complexing Agent [J]. Industrial & Engineering Chemistry Research, 2000, 39: 3907−3911.

[15] WANG Yi-ge, XIONG Ying, MENG Shu-lan, LI De-qian. Separation of yttrium from heavy lanthanide by CA-100 using the complexing agent [J]. Talanta, 2004, 63: 239−243.

[16] SUI Na, MIAO Shu-kai, CUI Kai-hui, MENG Fan-cheng, HUANG Kun. The interfacial “push and pull” competitive complexation and enhanced separation of praseodymium and neodymium [J]. Chemical Engineering Research and Design, 2023, 197: 85−95.

[17] MATSUYAMA H, OKAMOTO T, TERAMOTO M. Kinetic studies of exchange reactions between rare earth metal ions and their diethylenetriaminepentaacetic acid complexes [J]. Journal of Chemical Engineering of Japan, 1989, 22: 460−468.

[18] NILSSON M, NASH K L. Review article: A review of the development and operational characteristics of the TALSPEAK process [J]. Solvent Extraction and Ion Exchchange, 2007, 25: 665−701.

[19] SULLIVAN J C, NASH K L, CHOPPIN G R. A kinetic study of americium(III) and frans-1,2-diaminocyclohexane-tetraacetate [J]. Inorganic Chemistry, 1978, 17: 3374−3377.

[20] GENNARO M C, MIRTI P, CASALINO C. NMR study of intramolecular processes in EDTA metal complexes [J]. Polyhedron, 1983, 2: 13−18.

[21] NASH K L, BRIGHAM D, SHEHEE T C, MARTIN A. The kinetics of lanthanide complexation by EDTA and DTPA in lactate media [J]. Dalton Transactions, 2012, 41: 14547−14556.

[22] XUE Yun-long, TANG Zhi-yong, XU Wan-fu, ZOU Hai-kui, CHU Guang-wen, SUN Bao-chang, ZHANG Liang-liang, CHEN Jian-feng. Kinetics of the homogenous diazotization of p-nitroaniline with nitrous acid solution using stopped-flow technique [J]. Chemical Engineering Journal, 2021, 423: 130223.

[23] LIU He-lei, XIAO Min, LIANG Zhi-wu, RONGWONG W, LI Jie, TONTIWACHWUTHIKUL P. Analysis of reaction kinetics of CO_2 absorption into a novel 1-(2-hydroxyethyl)-piperidine solvent using stopped-flow technique [J]. Industrial & Engineering Chemistry Research, 2015, 54: 12525−12533.

[24] LI Jie, LIU He-lei, LIANG Zhi-wu, LUO Xiao, LIAO Hui-ying, IDEM R, TONTIWACHWUTHIKUL P. Experimental study of the kinetics of the homogenous reaction of CO_2 into

a novel aqueous 3-diethylamino-1,2- propanediol solution using the stopped-flow technique [J]. Chemical Engineering Journal, 2015, 270: 485−495.
[25] SONG De-an, LIU Hui-juan, QIANG Zhi-min, QU Jiu-hui. Determination of rapid chlorination rate constants by a stopped-flow spectrophotometric competition kinetics method [J]. Water Research, 2014, 55: 126−132.
[26] SUI Na, MIAO Shu-kai, CUI Kai-hui, MENG Fan-cheng, HUANG Kun. Non-equilibrium kinetic separation of thulium, yttrium and erbium on the surface of freely rising oil droplet [J]. Journal of Rare Earths, 2024, 42: 200−209.
[27] PAFFENROTH R, VRAJITORU D. DataViewer: A scene graph based visualization tool [C]//Proceedings 20th Eurographics UK Conference. Leicester, England: IEEE Computer Society, 2002: 147−148.
[28] SPOEL D V D, LINDAHL E, HESS B, GROENHOF G, MARK A E, BERENDSEN H J C. GROMACS: Fast, flexible, and free [J]. Journal of Computational Chemistry, 2005, 26: 1701−1718.
[29] MARTINEZ L, ANDRADE R, BIRGIN E G, MARTINEZ J M. PACKMOL: A package for building initial configurations for molecular dynamics simulations [J]. Journal of Computational Chemistry, 2009, 30: 2157−2164.
[30] KAMINSKI G A, FRIESNER R A, TIRADO-RIVES J, JORGENSEN W L. Evaluation and reparametrization of the OPLS-AA force field for proteins via comparison with accurate quantum chemical calculations on peptides [J]. Journal of Physical Chemistry B, 2001, 105: 6474−6487.
[31] CADENA C, MAGINN E J. Molecular simulation study of some thermophysical and transport properties of triazolium-based ionic liquids [J]. Journal of Physical Chemistry B, 2006, 110: 18026−18039.
[32] LI Peng-fei, MERZ K M. Taking into account the ion-induced dipole interaction in the nonbonded model of ions [J]. Journal of Chemical Theory Computation, 2014, 10: 289−297.
[33] HOOVER W G. Canonical dynamics: Equilibrium phase-space distributions [J]. Physical Review A, 1985, 31: 1695−1697.
[34] NOSÉ S. A unified formulation of the constant temperature molecular dynamics methods [J]. Journal of Chemical Physics, 1984, 81: 511−519.
[35] PARRINELLO M, RAHMAN A. Polymorphic transitions in single crystals: A new molecular dynamics method [J]. Journal of Applied Physics, 1981, 52: 7182−7190.
[36] MATSUYAMA H, KOMORI K, TERAMOTO M. Selectivity enhancement in the permeation of rare earth metals through supported liquid membranes by addition of diethylenetriaminepentaacetic acid to the aqueous phase [J]. Journal of Membrance Science, 1989, 47: 217−228.
[37] SUI Na, HUANG Kun, ZHANG Chao, WANG Ning, WANG Fu-chun, LIU Hui-zhou. Light, middle, and heavy rare-earth group separation: A new approach via a liquid-liquid-liquid three-phase system [J]. Industrial & Engineering Chemistry Research, 2013, 52: 5997−6008.
[38] GANDOLFO F, AMORELLO D, ROMANO V, ZINGALES R. Complex formation of the uranyl (UO_2^{2+}) ion with the diethylene triaminopentaacetate (DTPA) ligand at 25 °C in 3 M sodium perchlorate [J]. Journal of Chemical and Engineering Data, 2011, 56: 2110−2118.
[39] BECK M T. Critical evaluation of equilibrium constants in solution. Stability constants of metal complexes [J]. Pure and Applied Chemistry, 1977, 49: 127−135.
[40] RIDDELL F G. Structure, conformation, and mechanism in the membrane transport of alkali metal ions by ionophoric antibiotics [J]. Chirality, 2002, 14: 121−125.
[41] HERLNG J G, MOREL F M. Kinetics of trace metal complexation: Role of alkaline-earth metals [J]. Environmental Science & Technology, 1988, 22: 1469−1478.
[42] SMITH R, MARTELL A, MOTEKAITOS R. NIST critically selected stability constants of metal complexes database Version 8.0 [M]//NIST standard reference database 46. Gaithersburg, MD 20899, 2004.
[43] BYRNE R H, LI Bi-qiong. Comparative complexation behavior of the rare earths [J]. Geochimica et Cosmochimica Acta, 1995, 59: 4575−4589.

DTPA 配合动力学诱导 P507 强化分离钇、铒和铥

隋 娜[1,2]，苗书凯[1]，沈 昊[1]，崔凯辉[1]，王佳琦[1]，黄 焜[1]

1. 北京科技大学 冶金与生态工程学院，北京 100083；
2. 自然资源部 离子型稀土资源与环境重点实验室，赣州 341000

摘 要：基于非平衡动力学萃取技术，研究了采用不同的二乙三胺五乙酸(DTPA)添加顺序时稀土离子与 DTPA 的配合动力学。结果表明，在萃取开始时加入 DTPA，稀土 Tm/Er 和 Y/Er 之间的分离系数均高于萃取前预先加入 DTPA 时对应的分离系数。稀土 Y、Er、Tm 离子的萃取顺序为 Tm>Y>Er。通过停留光谱法从正向配合物形成速率和逆向配合物解离速率上查明了 Y、Er、Tm 离子与 DTPA 配合动力学差异的本质和动力学强化分离机理。研究发现，表观配合速率常数随着水溶液 pH 的增加逐渐降低，而随着 DTPA 浓度的增加而逐渐增加。根据计算得到的 Y、Er、Tm 在不同 pH 值下的反应动力学常数，验证了萃取优先顺序为 Tm>Y>Er。

关键词：稀土；萃取；配合动力学；二乙三胺五乙酸(DTPA)；停留光谱法

(Edited by Bing YANG)